Available online at www.sciencedirect.com
SCIENCE DIRECT®
Journal of Catalysis 220 (2003) 23–34
JOURNAL OF CATALYSIS
www.elsevier.com/locate/jcat

Theoretical study of propene metathesis proceeding on monomeric Mo centers of molybdena–alumina catalysts

Jarosław Handzlik

Institute of Organic Chemistry and Technology, Cracow University of Technology, ul. Warszawska 24, PL 31-155 Kraków, Poland

Received 24 December 2002; revised 30 May 2003; accepted 2 June 2003

Abstract

Density functional theory study of propene metathesis proceeding on monomeric Mo–alkylidene centers of molybdena–alumina catalysts is reported. Calculations have been carried out with the Gaussian 98 program, using the hybrid B3LYP functional. The applied models of active Mo sites are bonded to alumina clusters including two or four aluminum atoms. According to the calculations, two kinds of the molybdacyclobutane intermediates play a role in the mechanism of propene metathesis: one with trigonal bipyramidal geometry and the second with a square pyramidal structure. The latter intermediate is formed from the former and this reaction competes with the decomposition of the trigonal bipyramidal molybdacyclobutane to the Mo–alkylidene center and alkene. Both *syn* and *anti* rotational isomers of Mo–ethylidene centers have been considered and their reactivities toward propene are almost the same.

Keywords: Molybdena–alumina; Catalyst; Propene; Metathesis; DFT; Gaussian; Molybdacyclobutane

1. Introduction

A heterogeneous catalyst of olefin metathesis usually consists of a transition metal compound deposited on a high-surface-area support [1,2]. A commonly accepted carbene mechanism of homogeneous olefin metathesis [1,3,4] has been adopted to the heterogeneous catalytic systems [1,2,5–15]. According to this mechanism, surface metal–alkylidene species react with alkene molecules giving intermediate molybdacyclobutane complexes that decompose to new alkylidenes and the reaction products. In Fig. 1, an example scheme of propene metathesis is presented.

There is some experimental evidence of the existence of metal–alkylidene and metallacyclobutane species on the surface of the heterogeneous catalysts [11–13]. These centers can be formed after the catalyst is brought into contact with alkene [1,2,6,7] or cycloalkane [12–15]. Metal–alkylidene compounds have also been immobilized on the carrier [16–18].

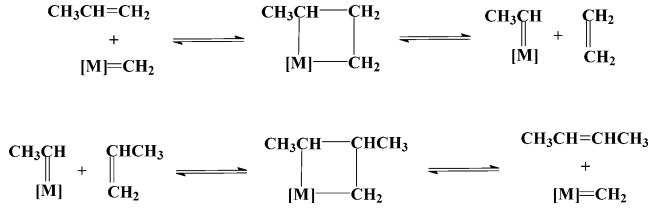

Fig. 1. Catalytic cycle of propene metathesis.

Several theoretical investigations of olefin metathesis [19–28] were reported; however, they are focused on the homogeneous systems. In the case of Mo–alkylidene Schrock-type catalysts, $Mo(NH)(CHR)(L)_2$ (R = H, CH_3; L = OH, OCH_3, OCF_3) complexes were applied as the model catalysts [23–25]. On the basis of DFT studies, it was predicted that the molybdacyclobutane intermediates have a trigonal bipyramidal (TBP) or square pyramidal (SP) geometry. The SP structure of the molybdacyclobutane complex with the electron-donating L ligands was shown to be more stable than the corresponding TBP structure [23,25]. In the case of the catalyst with the electron-withdrawing L ligands, the TBP intermediate was predicted to be more stable than the SP one [23] or the relative stabilities of the two molybdacyclobutane structures were reported to be dependent on the theoretical method applied [25]. However, it was pro-

E-mail address: jhandz@usk.pk.edu.pl.

0021-9517/$ – see front matter
doi:10.1016/S0021-9517(03)00268-9

posed in the latter work that the TBP structure is initially formed from the alkylidene complex and alkene, independently on the electronic properties of the L ligands. These results are generally consistent with the reported experimental investigations concerning $Mo(CHR)(NAr)(OR')_2$ and $W(CHR)(NAr)(OR')_2$ catalysts of olefin metathesis [29,30]. The metallacyclobutane complexes that had TBP or SP geometry, depending on the kind of the L ligands, were described. It was also proposed that olefin addition to the Mo–alkylidene complex yields the initial TBP metallacyclobutane, which can rearrange by a Berry-type pseudorotation to the SP structure [29].

DFT calculations of $Mo(O)(L)_2(C_3H_6)$ (L = Cl, OCH_3, OCF_3) molybdacyclobutanes showed that the SP structure was more stable than the TBP one in every studied case [23].

In contrast to the homogeneous systems, the structures of the surface alkylidene centers are not unambiguously determined. In the case of the monomeric centers of supported Mo catalysts, a distorted tetrahedral site with one oxo ligand, one alkylidene ligand, and two oxygen atoms connecting the molybdenum atom with the carrier was proposed [10,12–15,31,32]. Distorted tetrahedral dioxo Mo^{VI} species or their reduced forms can be the precursors of these monomeric Mo–alkylidene sites [10,12–15,31–33]. The presence of pseudo-tetrahedral monomeric Mo^{VI} centers was experimentally proved for the supported Mo catalysts [33–51]. These centers were often proposed to be dioxo species [33,41–52]. On the other hand, there were also reported experimental evidence for the existence of monooxo, not dioxo, surface monomeric Mo^{VI} species under dehydrated conditions [53–57].

In previous works [58–60], DFT investigations of ethene metathesis proceeding on molybdena–alumina catalyst were performed, applying the cluster model approach [61,62]. It was suggested that the active alkylidene sites did not contain Mo^{IV}, because of high activation barriers of some steps of the catalytic cycle involving a Mo^{IV} methylidene center [59]. In the case of the Mo^{VI} methylidene complex, the transition structure leading to the TBP molybdacyclobutane, as well as the transition state of the rearrangement of the TBP intermediate to the SP one, was localized [60]. It was shown that the conversion of the TBP molybdacyclobutane to the SP one proceeded easier than the decomposition of the TBP intermediate to the Mo^{VI} methylidene and ethene.

Both in the previous works and in the present studies the usually suggested pseudo-tetrahedral Mo–alkylidene centers with the oxo spectator ligand were assumed as the catalyst models. These models are analogous to the pseudo-tetrahedral Schrock catalysts.

In the present work, systematic DFT studies of the whole catalytic cycle of propene metathesis are performed. To the best of my knowledge, such theoretical investigations have not been reported so far, neither for homogeneous nor heterogeneous catalytic systems. The main aim of the current studies is a description of the details of the reaction mechanism and determination of the role of TBP and SP intermediates in the reaction kinetics.

2. Methods

In this study, the cluster approach was applied to model the surface active sites of propene metathesis. All calculations were carried out with Gaussian 98 program [63], using a hybrid B3LYP functional [64].

All the structures were optimized by applying the Berny algorithm and using redundant internal coordinates [65]. The LANL2DZ basis set was applied for geometry optimization. This basis set includes the Hay–Wadt effective core potential [66] plus double-zeta basis set (applied for Mo and Al) and Dunning–Huzinaga valence double-zeta set (D95V) on the first row (applied for C, H, and O). Harmonic vibration frequencies were calculated for each structure to confirm the potential energy minimum or the transition state involved and to obtain the zero-point energy (ZPE) values. The obtained transition structures were additionally verified by the IRC calculations [67,68].

Additionally, single-point energy calculations were performed using the D95V(d) basis sets for C and O, whereas Mo and Al were described by the LANL2DZ basis. This basis set combination is denoted here as LANL2DZ(d). If not stated otherwise, the presented energy differences were calculated according to the B3LYP/LANL2DZ(d)//B3LYP/LANL2DZ scheme. All presented energies are ZPE corrected.

The counterpoise method [69–71] was used to estimate the basis set superposition error (BSSE). The obtained BSSE values are reasonable and in the case of the transition states of alkene additions to the Mo–alkylidenes, they are in the range of 13–16 $kJ\,mol^{-1}$ (for the B3LYP/LANL2DZ calculations). However, the studied reactions should be considered in two directions which results in discontinuous potential surfaces if the BSSE corrections are consistently done [71]. For this reason, the energies reported in this work are not BSSE corrected. On the other hand, all presented energies are ZPE corrected.

All structures studied in this work are neutral. Two cluster models of alumina, a smaller one and a bigger one, were used to play a role of the carrier. The dangling bonds of the alumina clusters have been saturated with hydrogens. The vibrations of these hydrogens (excluding vibrations with imaginary frequencies) are included in the ZPE values, assuming that their contributions are canceled when the relative energies are calculated.

The structures applying the smaller cluster of alumina were fully optimized to make localization of transition states easier. The optimized geometry of the alumina part of these models was hardly changed, when going from one structure to another. For instance, the Al–Al distance differs maximally by less than 0.07 Å. In the case of the active sites models containing the larger alumina cluster, only the first

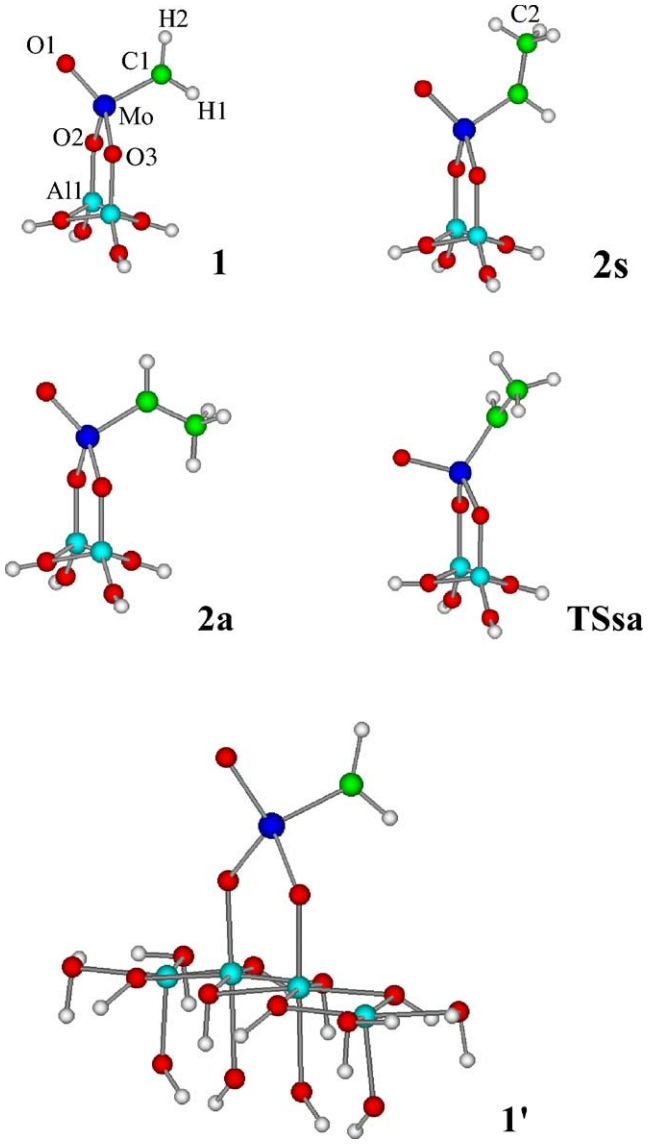

Fig. 2. Optimized structures of the cluster models of Mo^{VI} alkylidene centers and the transition state of the *syn* to *anti* conversion.

layer of the alumina part was allowed to be relaxed during geometry optimization, whereas the positions of the second-layer oxygens and all hydrogens were frozen. Before geometry optimization, each hydrogen was placed 0.97 Å from the oxygen, in the direction of the removed Al atom.

3. Results and discussion

3.1. Cluster models of surface Mo–alkylidenes

In the previous works [58–60], a model (**1**) of a monomeric Mo–methylidene center on alumina was proposed and applied (Fig. 2). This pseudo-tetrahedral structure having one oxo ligand and connected with two aluminum atoms is quite similar to the very effective four-coordinate $Mo(NAr)(CHR)(L)_2$ Schrock catalysts, if one takes into account that the =O ligand in **1** corresponds to the =NAr

Table 1
Selected geometrical parameters[a] of the Mo–alkylidene structures

	1	**2s**	**2a**	**1′**
Mo–C1	1.901	1.904	1.908	1.918
Mo–O1	1.726	1.728	1.728	1.741
Mo–O2	1.905	1.914	1.913	1.880
O2–Al1	1.765	1.762	1.762	1.840
C1–H1	1.096	1.103	–	1.096
C1–H2	1.092	–	1.095	1.093
Mo–C1–H1	119.8	112.4	–	119.2
Mo–C1–H2	124.0	–	119.4	124.4
Mo–C1–C2	–	132.0	124.5	–
O1–Mo–C1	104.0	103.1	103.6	104.3
O2–Mo–O3	96.8	96.8	96.7	99.4

[a] Bond lengths are given in Å, angles in degrees.

one. The small alumina cluster model included in **1** was previously examined [59]. It was shown that the properties (deprotonation energy and charge) of the two OH groups that are replaced by the alkylidene center in **1** are similar to the properties of the OH groups connected with octahedrally coordinated aluminum of a much bigger model of the (100) face of alumina. Moreover, the geometry of the four-membered ring of the small alumina cluster is very similar to the geometry of the corresponding fragment of the (100) plane of γ-alumina, if one takes into account the position of the atoms rather than their coordination. The geometry of the tetrahedral Al sites on the (110) crystal surface of alumina is quite different. Therefore, despite the fact that aluminum in **1** is tetrahedrally coordinated, it can be assumed that this small alumina cluster mimics octahedral aluminum centers with basic OH groups.

As far as Mo–ethylidene centers are concerned, two rotational isomers, *syn* (**2s**) and *anti* (**2a**), can be distinguished (Fig. 2). Both optimized species have distorted tetrahedral structures and possess C_s symmetry, similar to **1**. In Table 1, selected geometrical parameters of the Mo–alkylidene models are presented. The obtained geometries are consistent with the structures of four-coordinated Mo–alkylidene catalysts, determined both experimentally [29] and theoretically [23,25,72,73]. The reported value of the Mo=C bond in a Schrock-type complex is 1.880 Å [29]. It is close to the values of the carbene bond obtained in the present work (Table 1).

In the case of the *syn*-Mo–ethylidene center **2s** there is a significant difference between the Mo–C–H angle (112°) and the Mo–C–C one (132°). Moreover, the C–H bond distance in **2s** is a little increased, compared to other Mo–alkylidenes. This suggests the existence of a small agostic interaction between the Mo and the C–H bond in the *anti* position, which was also reported for $Mo(NH)(CHR)(L)_2$ complexes [25].

The *anti* rotamer (**2a**) is less stable than the *syn* one (**2s**); however, the predicted energy difference of 2 $kJ\,mol^{-1}$ is very small. On the other hand, the calculated activation energy of the rotation of the ethylidene moiety from the *anti* position to the *syn* one is relatively high, of the order of

Table 2
The experimental [12,13] and calculated wavenumbers of the C–H-stretching vibrations

	ν_{exp} (cm^{-1})		ν_{calc} (cm^{-1})	ν_{calc}[a] (cm^{-1})
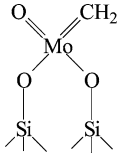		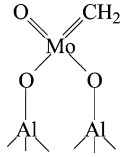	**1**	**1**
	3080		3225	3069
	2945		3096	2946
			1′	**1′**
			3211	3056
			3087	2938
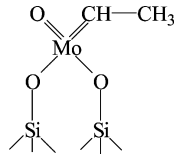		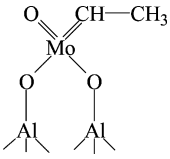	**2s**	**2s**
	2985		3143	2991
	2910		3070	2921
	2890		3052	2904
	2850		3007	2861

[a] 0.9516 scaling factor was applied.

75 kJ mol^{-1}. This value is in the range of reported experimental activation enthalpies for *anti* to *syn* conversions of Mo(NAr)(CHR)$(L)_2$ complexes with electron-withdrawing L ligands [74]. However, as will be shown later, the conversion of the *anti* rotamer to the *syn* one is more probable via propene metathesis than by the rotation of the ethylidene ligand. In Fig. 2, the geometry of the transition state (**TSsa**) of the *syn* to *anti* conversion is shown.

A second model (**1′**) of the Mo–methylidene center is also shown in Fig. 2. In this case, the larger cluster model of alumina was applied. This cluster, containing four aluminum atoms, was cut from the (100) surface of the crystal structure of γ-Al_2O_3 [75]. In Table 1, selected geometrical parameters of **1′** are presented. The pseudo-tetrahedral geometry of the Mo–methylidene center **1′** hardly differs from the geometry of **1**. The most significant difference can be noted in the case of the O–Al distance, which is 0.075 Å longer in **1′**. Consequently, the Mo–O2(O3) bonds in **1′** are shorter (by 0.025 Å), whereas the Mo–O1 and Mo–C1 distances are a little elongated (by 0.015 and 0.017 Å, respectively), in comparison to **1**. On the other hand, the angles are almost identical in both structures (Table 1).

There is little spectroscopic evidence for the existence of metal–carbene species on the surface of the olefin metathesis heterogeneous catalysts. Shelimov and co-workers [12,13] reported IR data of surface Mo–alkylidenes generated on molybdena–silica catalysts. In Table 2, the experimental wavenumbers of the C–H-stretching vibrations of the alkylidene moiety are compared with the corresponding frequencies calculated in the present work. Additionally, a scaling factor 0.9516, obtained by a least-squares fit of the calculated to the experimental vibrational frequencies, was used to recalculate the theoretical wavenumbers (the last column of Table 2). As can be seen, the vibrational frequencies calculated for the cluster models are very well consistent with the experimental data.

3.2. Propene metathesis

To enable a detailed study of the whole catalytic cycle of propene metathesis, the smaller cluster model of alumina was used. As Fig. 1 indicates, both Mo–methylidene and Mo–ethylidene centers are involved in the catalytic cycle.

Propene molecules can attack the Mo–methylidene center **1** in four different orientations. Two of them lead to a molybdacyclobutane intermediate with the methyl substituent connected to the carbon atom being in the opposite position to the molybdenum in the ring (Figs. 3A and B). The

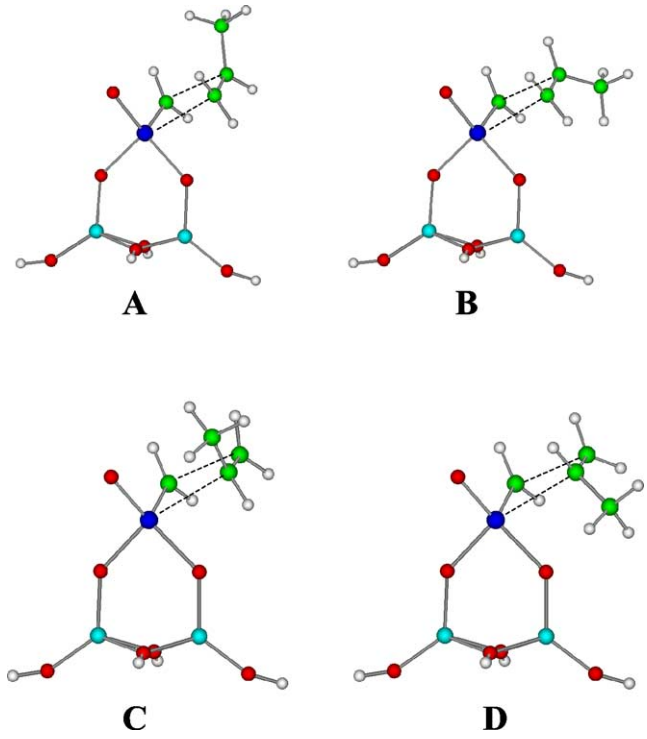

Fig. 3. Four possibilities of propene addition to the Mo–methylidene center **1**.

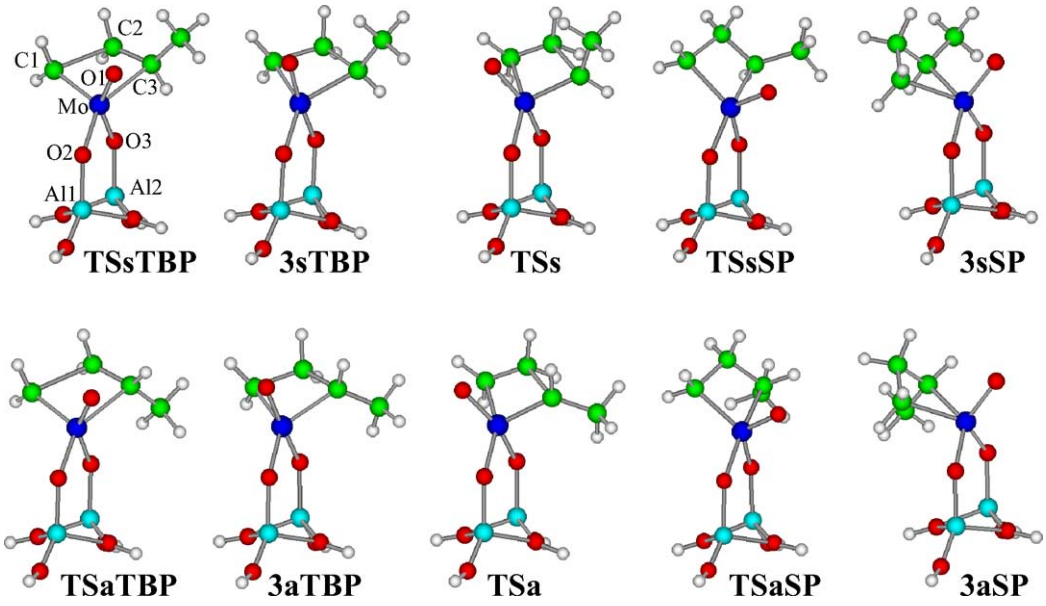

Fig. 4. Optimized structures of the minima and transition states involved in the pathways starting with propene addition to the Mo–methylidene center.

decomposition of such a molybdacyclobutane always gives another propene molecule and the molybdenamethylidene center. This case is called degenerate metathesis or nonproductive metathesis [1] and is not considered in the present work.

In the case of productive metathesis, there are two other possibilities of propene addition to **1**, both giving a molybdacyclobutane ring with the methyl group connected to the carbon atom adjacent to the molybdenum (Figs. 3C and D). The intermediate can decompose to ethene and the *syn*- or *anti*-Mo–ethylidene, depending on the orientation of the methyl substituent in the ring.

Structures corresponding to potential energy minima and transition states on the reaction path of propene addition to **1**, leading to the *syn*-Mo–ethylidene center **2s**, are shown in Fig. 4. In the first step, a molybdacyclobutane intermediate **3sTBP** with trigonal bipyramidal geometry is formed, via a transition state **TSsTBP**. The transition structure has a ring with the predicted Mo–C1–C3–C2 dihedral angle of about 169°. The ring of the **3sTBP** molybdacyclobutane is entirely flat. The O2, C1, and C3 atoms form the base of the trigonal bipyramid, whereas the O1 and O3 atoms are the vertexes. Geometry details of the presented structures are given in Table 3.

A significant Mo–C3 bond formation in the transition structure **TSsTBP** can be seen. The calculated Mo–C3 bond distance is 2.360 Å, whereas the final Mo–C3 bond distance in the **3sTBP** molybdacyclobutane is only by 0.268 Å shorter (Table 3). On the other hand, the predicted decrease of the C1–C2 bond length is much higher, of the order of 0.601 Å, when going from the transition state **TSsTBP** to the TBP molybdacyclobutane. Thus, the formation of the C1–C2 bond falls behind the Mo–C3 bond formation. Similar results were obtained in the case of ethene addition to the Mo–methylidene center [60].

Table 3
Selected geometrical parameters[a] of the transition states and intermediates for the pathway starting with the Mo–methylidene center and leading to the *syn*-Mo–ethylidene site

	TSsTBP	3sTBP	TSs	TSsSP	3sSP
Mo–C1	1.953	2.094	2.311	2.077	2.193
Mo–C3	2.360	2.092	1.961	2.189	2.208
Mo–O1	1.742	1.753	1.747	1.731	1.729
Mo–O2	1.924	1.898	1.926	1.911	1.912
Mo–O3	1.976	1.994	1.983	1.977	1.911
C1–C2	2.199	1.598	1.428	1.601	1.536
C2–C3	1.433	1.634	2.251	1.564	1.539
O2–Al1	1.749	1.762	1.750	1.774	1.762
O3–Al2	1.753	1.747	1.750	1.747	1.764
O2–Mo–O3	87.4	89.2	87.8	83.5	95.1
C1–Mo–C3	91.2	83.1	93.7	74.5	62.4
C1–C2–C3	115.2	118.5	114.4	109.4	95.6
Mo–C1–C3–C2	169.2	179.7	175.8	−152.3	−149.6

[a] Bond lengths are given in Å, angles in degrees.

To continue productive propene metathesis, the trigonal bipyramidal molybdacyclobutane **3sTBP** must decompose to the *syn*-molybdenaethylidene center **2s** and ethene. The transition state of this step, denoted as **TSs**, is shown in Fig. 4. It has an almost entirely flat ring with the Mo–C1–C3–C2 dihedral angle of 176°. Analogously to the **TSsTBP** structure, the Mo–C1 bond distance in **TSs** is less increased than the C2–C3 one, when going from the molybdacyclobutane intermediate to the transition structure (Table 3).

However, the trigonal bipyramidal intermediate **3sTBP** can also rearrange by a Berry-type pseudo-rotation to the molybdacyclobutane complex **3sSP** with square pyramidal geometry (Fig. 4). The base of the square pyramid is formed by O2, O3, C1, and C3 atoms, whereas the O1 atom is the vertex. The transition state for this transformation (**TSsSP**) possesses a bent ring with the Mo–C1–C3–C2 dihedral an-

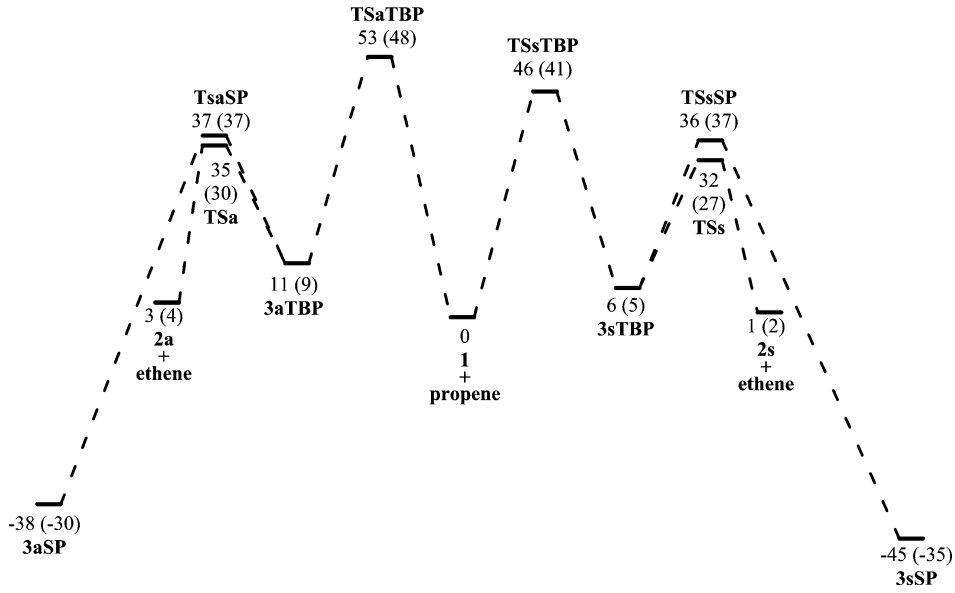

Fig. 5. Energy diagram of the pathways starting with propene addition to the Mo–methylidene center. The relative energies (kJ mol^{-1}) are obtained according to the B3LYP/LANL2DZ(d)//B3LYP/LANL2DZ and B3LYP/LANL2DZ (in parentheses) calculations.

gle of −152°. This is very close to −150°, the value of the Mo–C1–C3–C2 angle in the square pyramidal molybdacyclobutane **3sSP**. Among the C1, C2, and C3 atoms, C3 participates most in the motion corresponding to the imaginary frequency. The direction of the movement is opposite to the position of the methyl group. Consequently, both the Mo–C3 and the C2–C3 bond distances are not significantly different in the **TSsSP** and **3sSP** structures, whereas the Mo–C1 and C1–C2 bond lengths in **TSsSP** are hardly changed in comparison with the respective distances in **3sTBP** (Table 3).

In Fig. 4, structures corresponding to potential energy minima and transition states of the reaction path for propene addition to **1**, leading to the *anti*-Mo–ethylidene center **2a**, are also presented. Their geometry details are very similar to the respective data in Table 3 for the *syn* complex.

In Fig. 5, the energy diagram of propene addition to the Mo–methylidene center **1** is presented. The right side of the diagram corresponds to the reaction path leading to the *syn*-Mo–ethylidene complex **2s**, whereas the left side concerns the pathway leading to the *anti*-Mo-ethylidene structure **2a**.

In the case of the path leading to the *syn*-product, the predicted activation energy of propene addition to molybdenamethylidene center **1** is 46 kJ mol^{-1}. The calculated energy change for this reaction is 6 kJ mol^{-1}.

The predicted activation barrier of the conversion of **3sTBP** to the *syn*-Mo–ethylidene center **2s** and ethene is only 26 kJ mol^{-1} (Fig. 5). Conversion of the **3sTBP** intermediate to the square pyramidal one is exothermic ($\Delta E = -51$ kJ mol^{-1}) with the predicted activation barrier of only 4 kJ mol^{-1} higher than for the step leading to **2s** and ethene. However, the reverse transformation of **3sSP** to the TBP intermediate has a relatively high activation energy of 81 kJ mol^{-1}. Moreover, it seems that the SP molybdacyclobutane cannot decompose directly to the Mo–alkylidene center and alkene, while avoiding the TBP intermediate [25,29,60]. Several attempts were undertaken to localize a transitions state of a direct decomposition of the SP intermediate to the Mo–alkylidene center and alkene; however, they all failed. Thus, the possibility of the conversion of the TBP intermediate to the SP one is disadvantageous, because the reverse step, which is necessary to restore the metathesis active site, is endothermic with a relatively high activation barrier.

The transition state of the movement of **3sTBP** to **3sSP**, in the direction of the methyl substituent in the ring, has also been localized. The activation barrier is by about 3 kJ mol^{-1} higher than in the case of the rotation through the **TSsSP**.

The overall reaction of the Mo-methylidene center **1** with propene leading to the **2s** center and ethene has a very low energy change (1 kJ mol^{-1}), as can be expected for the double-bond metathesis. On the other hand, the overall formation of the square pyramidal intermediate **3sSP** from **1** and propene is clearly exothermic ($\Delta E = -45$ kJ mol^{-1}).

It is seen in Fig. 5 that the left side of the energy diagram, which concerns the pathway leading to the *anti*-Mo–ethylidene center, is very similar to the right side. The only significant difference is the energy barrier of propene addition to **1**. The barrier is 7 kJ mol^{-1} higher for the pathway leading to the *anti* rotamer. Therefore, the formation of the *syn* center during propene metathesis is more probable than the formation of the *anti* one, although one can predict that the *anti* center is also generated, by taking into account that the difference between the energy barriers is small.

In the decomposition pathways of the TBP intermediates both to the *syn* center and to the *anti* one, additional minima being ethene–molybdenaethylidene π-complexes have also been localized. However, these minima are very shallow. The

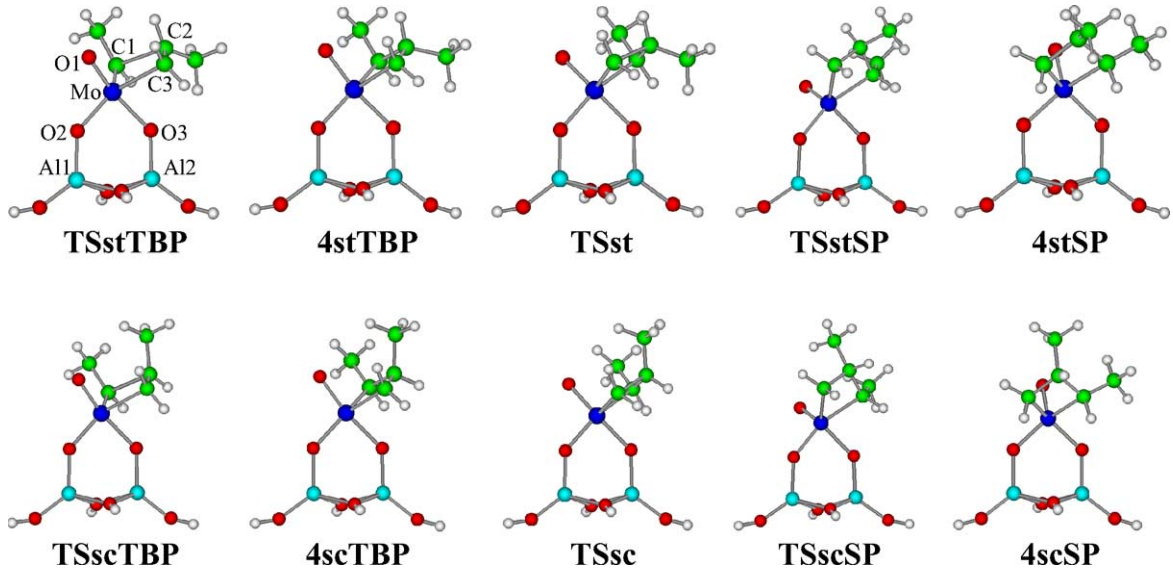

Fig. 6. Optimized structures of the minima and transition states involved in the pathways starting with propene addition to the *syn*-Mo–ethylidene center.

reactions of their decompositions to the corresponding Mo–ethylidene sites and infinitely distant ethene are exothermic, with almost zero activation barriers, if the energy without ZPE correction is taken into account. If the ZPE is added, the barriers become negative. For clarity, these π-complexes are not included in Figs. 4 and 5. In the case of interaction of propene or 2-butene with the Mo–alkylidene species, as well as the interaction of ethene with the Mo–methylidene center **1** [60], any analogous minima have not been localized.

To continue the catalytic cycle of propene metathesis (Fig. 1), propene addition to the Mo–ethylidene center must take place. As was noted in the case of the Mo–methylidene center, propene molecules can attack the Mo–ethylidene center (**2s**, **2a**) at four different positions. Two of them are the first steps of nonproductive metathesis that reproduces propene molecules. On the other hand, productive metathesis leads to *trans*-2-butene or *cis*-2-butene, depending on the mutual positions of methyl substituents in the molybdacyclobutane intermediate.

In Fig. 6, transition states and intermediates of the pathway starting with the *syn* center **2s** and leading to the *trans* and *cis* isomer are presented. The corresponding geometry details concerning the *trans* pathway are shown in Table 4.

In Fig. 7, the energy diagram of propene addition to **2s** is presented. The right side of the diagram corresponds to the pathway leading to *trans*-2-butene, whereas the left side concerns the pathway leading to the *cis* isomer. As we can see, the formation of the molybdacyclobutane intermediates (**4stTBP**, **4scTBP**) from the Mo–ethylidene center **2s** and propene is more endothermic ($\Delta E = 21$ and 28 kJ mol^{-1}, respectively) than the corresponding step starting with center **1**. The predicted activation energy of propene addition to the *syn*-Mo–ethylidene center on the reaction path leading to *trans*-2-butene is 42 kJ mol^{-1}. In the second case, the corresponding value is about 6 kJ mol^{-1} higher. However, the situation is different if we consider the decomposition of

Table 4
Selected geometrical parameters[a] of the transitions states and intermediates for the pathway starting with the *syn*-Mo–ethylidene center and leading to the *trans* product

	TSstTBP	4stTBP	TSst	TSstSP	4stSP
Mo–C1	1.966	2.088	2.336	2.195	2.207
Mo–C3	2.270	2.096	1.953	2.077	2.191
Mo–O1	1.748	1.753	1.742	1.731	1.729
Mo–O2	1.924	1.900	1.925	1.913	1.913
Mo–O3	1.991	1.995	1.980	1.974	1.911
C1–C2	2.196	1.641	1.442	1.566	1.541
C2–C3	1.445	1.600	2.204	1.601	1.537
O2–Al1	1.750	1.761	1.749	1.774	1.762
O3–Al2	1.750	1.747	1.753	1.749	1.764
O2–Mo–O3	87.6	89.0	87.0	83.6	95.1
C1–Mo–C3	91.8	82.5	90.4	74.0	62.2
C1–C2–C3	112.1	116.6	112.2	108.6	95.1
Mo–C1–C3–C2	175.3	−179.4	169.9	−155.1	−149.2

[a] Bond lengths are given in Å, angles in degrees.

the molybdacyclobutane intermediates (**4stTBP**, **4scTBP**) to the Mo–methylidene center **1** and 2-butene. At this step, the formation of *cis* isomer has the activation barrier about 5 kJ mol^{-1} lower than in the case of the *trans* isomer (Fig. 7). However, the conversion of the TBP intermediate to the SP one (the movement toward the carbon without the methyl substituent) has the activation barrier lower (Fig. 7). Similarly to the pathway presented in Fig. 5, these steps are also exothermic with the energy change of about −60 kJ mol^{-1}. Therefore, the reverse steps have relatively high activation barriers (Fig. 7). It is worth noting that in both cases, the activation barrier of propene addition to the Mo–ethylidene center is lower than the barrier of propene addition to the Mo–methylidene center **1** (Fig. 5).

In Fig. 8, transition states and intermediates concerning the pathway starting with the *anti*-Mo–ethylidene center **2a** and leading to *trans*- and *cis*-2-butene are shown. The ob-

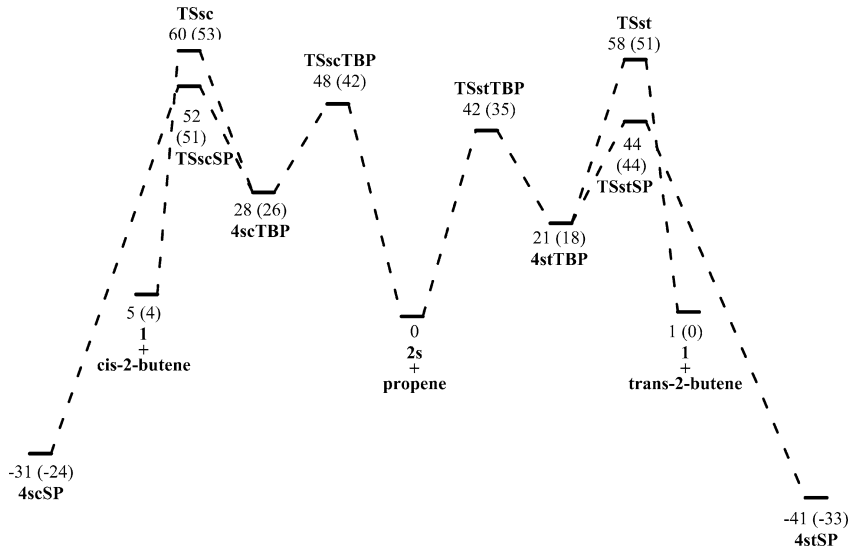

Fig. 7. Energy diagram of the pathways starting with propene addition to the *syn*-Mo–ethylidene center. The relative energies (kJ mol^{-1}) are obtained according to the B3LYP/LANL2DZ(d)//B3LYP/LANL2DZ and B3LYP/LANL2DZ (in parentheses) calculations.

tained structures are fully analogous to the geometries presented in Fig. 6.

In Fig. 9, an energy diagram of propene addition to the *anti*-Mo–ethylidene center is shown. The right and left sides of the diagram correspond to the pathway leading to *trans*-2-butene and *cis*-2-butene, respectively. As we can see, both pathways are very similar to the pathways of propene addition to the *syn*-Mo-ethylidene center (Fig. 7). Where the *anti* rotamer is concerned (Fig. 9), the predicted activation energy of the first step of the path leading to *cis*-2-butene is by 2 kJ mol^{-1} higher than for the pathway starting with the *syn* rotamer (Fig. 7). In the case of the pathways resulting in formation of *trans*-2-butene, the corresponding difference is hardly of about 1 kJ mol^{-1}. In the case of the pathway starting with the *syn* rotamer, the barrier of decomposition of the TBP intermediate to *trans*-2-butene is 4 kJ mol^{-1} lower than for pathway beginning with the *anti* one. The corresponding step leading to *cis*-2-butene has almost the same activation energy in both pathways (Figs. 7 and 9) but in the latter case (Fig. 9), the reaction is 7 kJ mol^{-1} more exothermic. However, according to the present calculations, one can generally conclude that the predicted reactivity of the *syn* and *anti* ro-

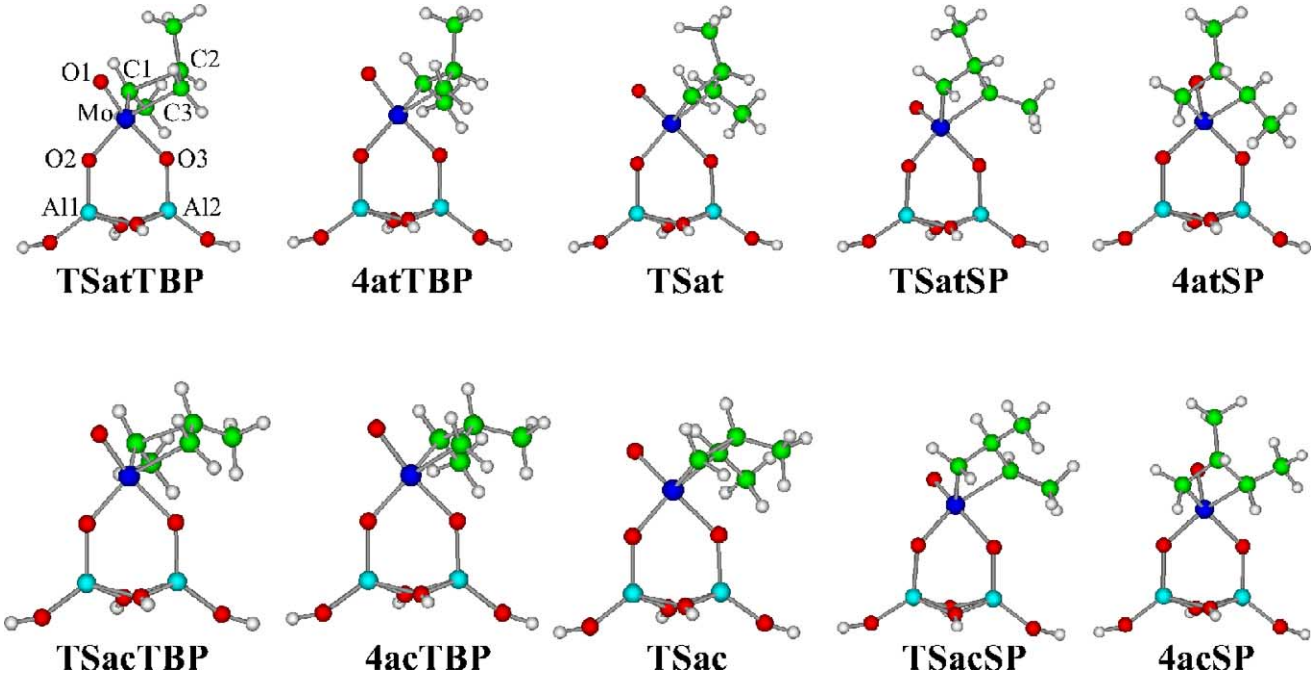

Fig. 8. Optimized structures of the minima and transition states involved in the pathways starting with propene addition to the *anti*-Mo–ethylidene center.

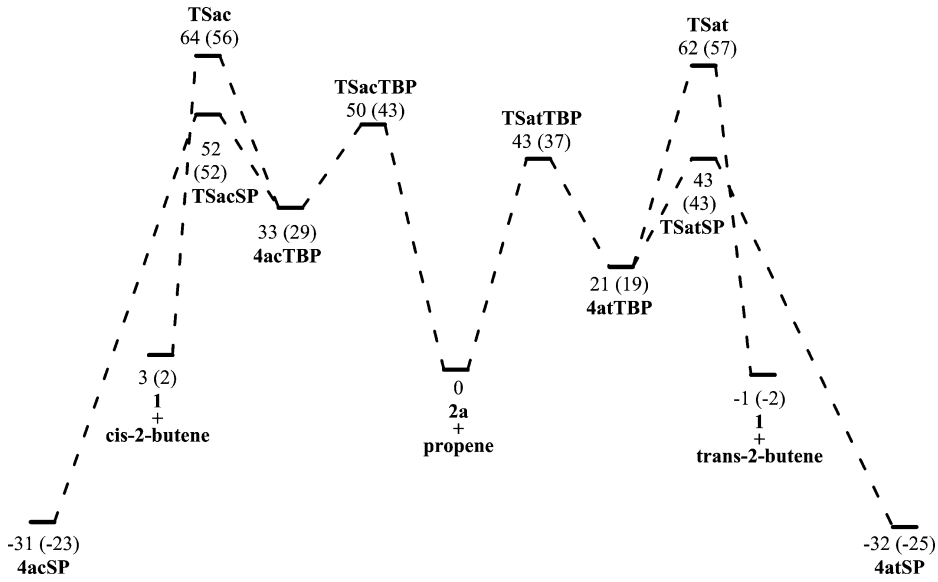

Fig. 9. Energy diagram of the pathways starting with propene addition to the *anti*-Mo–ethylidene center. The relative energies (kJ mol^{-1}) are obtained according to the B3LYP/LANL2DZ(d)//B3LYP/LANL2DZ and B3LYP/LANL2DZ (in parentheses) calculations.

tational isomers in propene metathesis is approximately the same. In all the cases of the transformations of the TBP intermediates to the SP structures, the movement toward the carbon that does not possess the methyl substituent has a barrier by 2–4 kJ mol^{-1} lower than in the case of the respective rotation in the opposite direction.

On the basis of the results obtained, it can be concluded that the decomposition of the square pyramidal molybdacyclobutane to the Mo–alkylidene center and the respective alkene occurs via the trigonal bipyramidal molybdacyclobutane. This is consistent with the previous calculations for ethene metathesis [60], as well as with the suggestions of Schrock and co-workers [29] and the theoretical results of Wu and Peng concerning homogeneous Mo catalysts [25]. According to the earlier theoretical studies of ethene metathesis [60], it can also be stated that the activation barriers of propene addition to the Mo–alkylidene centers are higher than the activation energy of ethene addition to the Mo–methylidene center ($\Delta E = 30$ kJ mol^{-1}, from the B3LYP/LANL2DZ calculations; however, in [60] values of ΔH°_{298}, not ΔE, were reported).

Many expressions, both macro- [32,76–79] and microkinetic [8,9,80,81], were applied to describe propene metathesis. The model based on the elementary steps of the carbene mechanism [8] seems to be the most accurate. In this model, the product desorption (or decomposition of the molybdacyclobutane intermediate) was shown to be the most likely rate-determining step [8]. It was proposed and experimentally confirmed [8,9] for the reaction proceeding on Re_2O_7/Al_2O_3 catalysts. The present calculations concerning the molybdena–alumina catalyst suggest that the kinetics of the process studied is somewhat more complex (Figs. 5, 7, and 9). Both possible structures of the molybdacyclobutane intermediates (TBP and SP) can play a role in the kinetics of the overall reaction.

3.3. Cross-metathesis of ethene and 2-butene

On the basis of the present results (Figs. 5, 7, and 9), cross-metathesis of ethene and 2-butene can also be discussed. As can be seen from Fig. 5, the predicted activation energies of ethene addition to both *syn* and *anti* Mo–ethylidene centers are about 25–26 kJ mol^{-1}, according to the B3LYP/LANL2DZ calculations (31–32 kJ mol^{-1} if LANL2DZ(d) basis set is used). This is less than the activation barrier for the cycloaddition of ethene with Mo–methylidene complexes (30 kJ mol^{-1}, according to the B3LYP/LANL2DZ calculations in [60]). The activation barriers for decomposition of the trigonal bipyramidal intermediates to the Mo–methylidene complex and propene are about 10 kJ mol^{-1} higher. They are also higher than the respective barriers of the undesirable conversion of the TBP structure to the SP one.

On the other hand, the activation energies of the cycloaddition of 2-butenes with the Mo–methylidene center are approximately three times as high as the corresponding energies of decomposition of the respective TBP molybdacyclobutanes to propene and the Mo–ethylidene complex (Figs. 7 and 9). The latter have activation barriers lower than the barriers of the corresponding transformations to the SP molybdacyclobutanes. One can also see that the *cis* reactant adds a little easier to the Mo–ethylidene center than the *trans* one.

Therefore, it depends on the reactant and the kind of the Mo–alkylidene center, which elementary step has the highest activation barrier in the given pathway. It is also predicted

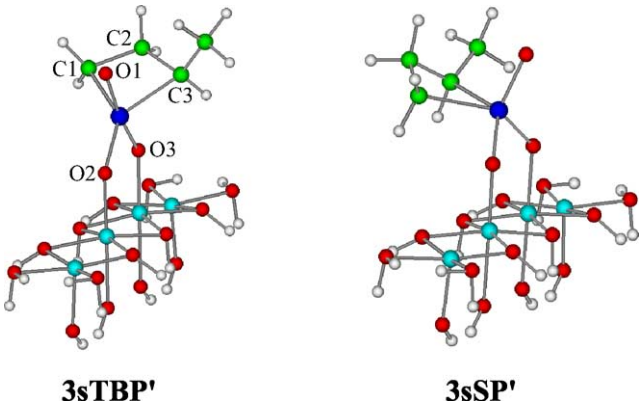

Fig. 10. Optimized structures of the TBP and SP molybdacyclobutanes involved in pathways starting with propene addition to the Mo–methylidene center—the larger cluster model.

that the shorter the alkene chain, the more facile its addition to the Mo–alkylidene center.

3.4. TBP and SP molybdacyclobutane intermediates—the larger cluster of alumina

The TBP and SP intermediates involved in the reaction path of propene addition to the Mo–methylidene center, leading to the *syn* product, also have been studied with application of the larger cluster of alumina. In Fig. 10, the structures of the **3sTBP′** and **3sSP′** molybdacyclobutanes are shown. Their selected geometrical parameters are collected in Table 5. Similarly to **1′** and **1**, the O–Al bonds in **3sTBP′** and **3sSP′** are elongated (0.061–0.080 Å) and Mo–O2(O3) distances are shorter (0.023–0.040 Å), compared to the respective structures attached to the smaller alumina cluster. The Mo–C and Mo–O1 bond lengths are less changed (0.009–0.023 Å).

The calculated energy change of the reaction: **1′** + $C_3H_6 \rightarrow$ **3sTBP′** is 38 kJ mol^{-1} (according to both B3LYP/LANL2DZ(d)//B3LYP/LANL2DZ and B3LYP/LANL2DZ calculations). This value is about 30 kJ mol^{-1} higher than in the case of the corresponding structures with the smaller alumina cluster (Fig. 5). On the other hand, the formation of the **3sSP′** molybdacyclobutane from **1′** and propene is exothermic and the predicted energy change is almost the same as in the case of the formation of **3sSP** (-46 kJ mol^{-1} from the B3LYP/LANL2DZ(d)//B3LYP/LANL2DZ calculations and -33 kJ mol^{-1} from the B3LYP/LANL2DZ calculations). Although the choice of the alumina cluster influences the relative energy of the TBP intermediate, it is very likely that the general picture of the reaction mechanism will not change with a change of the cluster model, as long as the transformation of the TBP molybdacyclobutane to the SP one competes with decomposition of the former one to the Mo–alkylidene center and alkene.

It is known that the percentage of the active metathesis sites is usually very low (less than 1% of the transition metal atoms) and their structure and localization is not unambiguously determined [1]. Although it is believed that the (110) plane of γ-Al_2O_3 is preferentially exposed, the mixture of the (110), (100), and (111) faces is often considered [82,83]. In this investigation, it has been assumed that the reaction proceeds on monomeric Mo centers, each connected with two octahedrally coordinated aluminum atoms of (100) alumina surface [59]. However, both other structures and other localization of the active sites are possible. For example, the active Mo–alkylidene centers can be formed in place of more acidic OH groups [1,84]. In such cases, the calculation results can be somewhat different, because the relative stabilities of the TBP and SP molybdacyclobutanes should be influenced by the local electronic properties of the carrier. The carrier is an equivalent of the alkoxy ligands of the homogeneous Schrock catalysts and it is known that the electronic properties of these ligands affect the relative stabilities of the TBP and SP molibdacyclobutane complexes [23,25,29]. Nevertheless, it seems that the complex picture of the kinetics of propene metathesis will be maintained in any case, because of the possible existence of different molybdacyclobutane intermediates that can rearrange each other.

Table 5
Selected geometrical parameters[a] of the TBP and SP molybdacyclobutanes for the pathway starting with the Mo–methylidene center and leading to the *syn*-Mo–ethylidene site—the larger cluster model

	3sTBP′	**3sSP′**
Mo–C1	2.110	2.204
Mo–C3	2.109	2.217
Mo–O1	1.776	1.741
Mo–O2	1.869	1.887
Mo–O3	1.954	1.888
C1–C2	1.600	1.539
C2–C3	1.628	1.541
O2–Al	1.833	1.842
O3–Al	1.808	1.842
O2–Mo–O3	92.3	97.4
C1–Mo–C3	82.0	62.4
C1–C2–C3	117.9	96.1
Mo–C1–C3–C2	179.1	−149.2

[a] Bond lengths are given in Å, angles in degrees.

4. Conclusions

In the present DFT investigation, the carbene mechanism of propene metathesis proceeding on monomeric Mo centers of molybdena–alumina catalysts has been studied. To enable a detailed study of the reaction paths, a simple cluster model of γ-alumina was used.

Based on the current calculations and the cluster models applied, it can be concluded that the mechanism of propene metathesis is more complex than is usually assumed in microkinetic models. As it was previously shown for ethene metathesis [60], two structures of the molybdacyclobutane intermediates are distinguished: TBP and SP. The former structure is the product of cycloaddition of the reactant with the Mo–alkylidene center, which can decompose to the prod-

uct and another Mo–alkylidene complex. The latter structure is formed directly from the former one and this transformation competes with the decomposition of the TBP molybdacyclobutane to the metathesis product. The decomposition of the SP molybdacyclobutane to the Mo–alkylidene center and alkene occurs via the TBP intermediate.

According to the results obtained, the reactivities of the *syn* Mo–ethylidene complex and the *anti* rotamer in propene metathesis are very similar.

The activation barriers of propene addition to the Mo–alkylidene centers are higher than those for ethene metathesis, whereas the predicted barrier of ethene addition to the Mo–ethylidene center is a little lower than in the case of its addition to the Mo–methylidene center during ethene metathesis. The activation energies of the cycloaddition of 2-butene with the Mo–methylidene center are the highest among the studied activation barriers of alkene additions to the Mo–alkylidene sites.

Further investigations applying larger cluster models and taking into account various possible localizations of the active sites on the carrier are in progress.

Acknowledgment

Computing resources from Academic Computer Centre CYFRONET UMM (SGI Origin2000 computer, Grant KBN/SGI_ORIGIN_2000/PK/109/1999) are gratefully acknowledged.

References

[1] K.J. Ivin, J.C. Mol, Olefin Metathesis and Metathesis Polymerization, Academic Press, London, 1997.
[2] J. Handzlik, J. Ogonowski, Metateza Olefin, Monografia, Seria Inżynieria i Technologia Chemiczna, Vol. 223, Politechnika Krakowska, Kraków, 1998.
[3] J.-L. Hèrisson, Y. Chauvin, Makromol. Chem. 141 (1971) 161.
[4] T.J. Katz, R. Rothchild, J. Am. Chem. Soc. 98 (1976) 2519.
[5] R.H. Grubbs, S.J. Swetnick, J. Mol. Catal. 8 (1980) 25.
[6] M.F. Farona, R.L. Tucker, J. Mol. Catal. 8 (1980) 85.
[7] J.R. McCoy, M.F. Farona, J. Mol. Catal. 66 (1991) 51.
[8] F. Kapteijn, H.L.G. Bredt, E. Homburg, J.C. Mol, Ind. Eng. Chem. Prod. Res. Dev. 20 (1981) 457.
[9] V.G. Gomes, O.M. Fuller, AIChE J. 42 (1996) 204.
[10] Y. Iwasawa, H. Kubo, H. Hamamura, J. Mol. Catal. 28 (1985) 191.
[11] B.N. Shelimov, I.V. Elev, V.B. Kazansky, J. Mol. Catal. 46 (1988) 187.
[12] K.A. Vikulov, I.V. Elev, B.N. Shelimov, V.B. Kazansky, J. Mol. Catal. 55 (1989) 126.
[13] K.A. Vikulov, B.N. Shelimov, V.B. Kazansky, J. Mol. Catal. 65 (1991) 393.
[14] K.A. Vikulov, B.N. Shelimov, V.B. Kazansky, J. Mol. Catal. 72 (1992) 1.
[15] K.A. Vikulov, B.N. Shelimov, V.B. Kazansky, J.C. Mol, J. Mol. Catal. 90 (1994) 61.
[16] S.T. Nguyen, R.H. Grubbs, J. Organomet. Chem. 497 (1995) 195.
[17] P. Preishuber-Pflügl, P. Buchacher, E. Eder, R.M. Schitter, F. Stelzer, J. Mol. Catal. A 133 (1998) 151.
[18] S.I. Wolke, R. Buffon, J. Mol. Catal. A 160 (2000) 181.
[19] A.K. Rappé, W.A. Goddard III, J. Am. Chem. Soc. 102 (1980) 5114.
[20] A.K. Rappé, W.A. Goddard III, J. Am. Chem. Soc. 104 (1982) 448.
[21] E.V. Anslyn, W.A. Goddard III, Organometallics 8 (1989) 1550.
[22] M. Sodupe, J.M. Lluch, A. Oliva, J. Bertrán, J. Mol. Struct. (Theochem.) 251 (1991) 37.
[23] E. Folga, T. Ziegler, Organometallics 12 (1993) 325.
[24] H.H. Fox, M.H. Schofield, R.R. Schrock, Organometallics 13 (1994) 2804.
[25] Y.-D. Wu, Z.-H. Peng, J. Am. Chem. Soc. 119 (1997) 8043.
[26] O.M. Aagaard, R.J. Meier, F. Buda, J. Am. Chem. Soc. 120 (1998) 7174.
[27] R.J. Meier, O.M. Aagaard, F. Buda, J. Mol. Catal. A 160 (2000) 189.
[28] C. Adlhart, C. Hinderling, H. Baumann, P. Chen, J. Am. Chem. Soc. 122 (2000) 8204.
[29] G.C. Bazan, E. Khosravi, R.R. Schrock, W.J. Feast, V.C. Gibson, M.B. O'Regan, J.K. Thomas, W.M. Davis, J. Am. Chem. Soc. 112 (1990) 8378.
[30] J. Feldman, R.R. Schrock, in: S.J. Lippard (Ed.), Progress in Inorganic Chemistry, Vol. 39, Wiley, New York, 1991, p. 1.
[31] M. Anpo, M. Kondo, Y. Kubokawa, C. Louis, M. Che, J. Chem. Soc., Faraday Trans. 1 84 (1988) 2771.
[32] W. Grünert, A.Yu. Stakheev, R. Feldhaus, K. Anders, E.S. Shpiro, Kh.M. Minachev, J. Catal. 135 (1992) 287.
[33] T. Ono, M. Anpo, Y. Kubokawa, J. Phys. Chem. 90 (1986) 4780.
[34] H. Jeziorowski, H. Knözinger, J. Phys. Chem. 83 (1979) 1166.
[35] K. Marcinkowska, L. Rodrigo, S. Kaliaguine, P.C. Roberge, J. Catal. 97 (1986) 75.
[36] H. Shimada, N. Matsubayashi, T. Sato, Y. Yoshimura, A. Nishijima, J. Catal. 138 (1992) 746.
[37] H. Hu, I.E. Wachs, S.R. Bare, J. Phys. Chem. 99 (1995) 10897.
[38] S. Imamura, H. Sasaki, M. Shono, H. Kanai, J. Catal. 177 (1998) 72.
[39] G. Xiong, C. Li, Z. Feng, P. Ying, Q. Xin, J. Liu, J. Catal. 186 (1999) 234.
[40] R. Radhakrishnan, C. Reed, S.T. Oyama, M. Seman, J.N. Kondo, K. Domen, Y. Ohminami, K. Asakura, J. Phys. Chem. B 105 (2001) 8519.
[41] Y. Iwasawa, Y. Nakano, S. Ogasawara, J. Chem. Soc., Faraday Trans. 1 74 (1978) 2968.
[42] Y. Iwasawa, S. Ogasawara, J. Chem. Soc., Faraday Trans. 1 75 (1979) 1465.
[43] D.S. Zingg, L.E. Makovsky, R.E. Tischer, F.R. Brown, D.M. Hercules, J. Phys. Chem. 84 (1980) 2898.
[44] Y. Iwasawa, Y. Sato, H. Kuroda, J. Catal. 82 (1983) 289.
[45] Y. Iwasawa, M. Yamagishi, J. Catal. 82 (1983) 373.
[46] Y. Okamoto, T. Imanaka, J. Phys. Chem. 92 (1988) 7102.
[47] M. Anpo, M. Kondo, S. Coluccia, C. Louis, M. Che, J. Am. Chem. Soc. 111 (1989) 8791.
[48] A.N. Desikan, L. Huang, S.T. Oyama, J. Phys. Chem. 95 (1991) 10050.
[49] C. Louis, M. Che, M. Anpo, J. Catal. 141 (1993) 453.
[50] Y. Iizuka, M. Sanada, J. Tsunetoshi, J. Furukawa, A. Kumao, S. Arai, K. Tomishige, Y. Iwasawa, J. Chem. Soc., Faraday Trans. 92 (1996) 1249.
[51] S. Takenaka, T. Tanaka, T. Funabiki, S. Yoshida, J. Phys. Chem. B 102 (1998) 2960.
[52] B.M. Reddy, B. Chowdhury, P.G. Smirniotis, Appl. Catal. A 211 (2001) 19.
[53] A.N. Desikan, L. Huang, T. Oyama, J. Chem. Soc., Faraday Trans. 88 (1992) 3357.
[54] M.A. Vuurman, I.E. Wachs, J. Phys. Chem. 96 (1992) 5008.
[55] D.S. Kim, I.E. Wachs, K. Segawa, J. Catal. 146 (1994) 268.
[56] M.A. Bañares, H. Hu, I.E. Wachs, J. Catal. 150 (1994) 407.
[57] B.M. Weckhuysen, J.-M. Jehng, I.E. Wachs, J. Phys. Chem. B 104 (2000) 7382.
[58] J. Handzlik, J. Ogonowski, in: A. Corma, F.V. Melo, S. Mendioroz, J.L.G. Fierro (Eds.), Stud. Surf. Sci. Catal., Vol. 130, Elsevier, Amsterdam, 2000, p. 1181.
[59] J. Handzlik, J. Ogonowski, J. Mol. Catal. A 175 (2001) 215.

[60] J. Handzlik, J. Ogonowski, J. Mol. Catal. A 184 (2002) 371.
[61] R.A. van Santen, J. Mol. Catal. A 115 (1997) 405.
[62] C.R.A. Catlow, L. Ackermann, R.G. Bell, F. Corà, D.H. Gay, M.A. Nygren, J.C. Pereira, G. Sastre, B. Slater, P.E. Sinclair, Faraday Discuss. 106 (1997) 1.
[63] M.J. Frisch, G.W. Trucks, H.B. Schlegel, G.E. Scuseria, M.A. Robb, J.R. Cheeseman, V.G. Zakrzewski, J.A. Montgomery, Jr., R.E. Stratmann, J.C. Burant, S. Dapprich, J.M. Millam, A.D. Daniels, K.N. Kudin, M.C. Strain, O. Farkas, J. Tomasi, V. Barone, M. Cossi, R. Cammi, B. Mennucci, C. Pomelli, C. Adamo, S. Clifford, J. Ochterski, G.A. Petersson, P.Y. Ayala, Q. Cui, K. Morokuma, P. Salvador, J.J. Dannenberg, D.K. Malick, A.D. Rabuck, K. Raghavachari, J.B. Foresman, J. Cioslowski, J.V. Ortiz, A.G. Baboul, B.B. Stefanov, G. Liu, A. Liashenko, P. Piskorz, J. Komaromi, R. Gomperts, R.L. Martin, D.J. Fox, T. Keith, M.A. Al-Laham, C.Y. Peng, A. Nanayakkara, M. Challacombe, P.M.W. Gill, B. Johnson, W. Chen, M.W. Wong, J.L. Andres, C. Gonzalez, M. Head-Gordon, E.S. Replogle, J.A. Pople, Gaussian 98, revision A.11, Gaussian, Inc., Pittsburgh, PA, 2001.
[64] A.D. Becke, J. Chem. Phys. 98 (1993) 5648.
[65] C. Peng, P.Y. Ayala, H.B. Schlegel, M.J. Frisch, J. Comput. Chem. 17 (1996) 49.
[66] P.J. Hay, W.R. Wadt, J. Chem. Phys. 82 (1985) 299.
[67] C. Gonzalez, H.B. Schlegel, J. Chem. Phys. 90 (1989) 2154.
[68] C. Gonzalez, H.B. Schlegel, J. Phys. Chem. 94 (1990) 5523.
[69] S.F. Boys, F. Bernardi, Mol. Phys. 19 (1970) 553.
[70] F.B. van Duijneveldt, J.G.C.M. van Duijneveldt-van de Rijdt, J.H. van Lenthe, Chem. Rev. 94 (1994) 1873.
[71] G. Lendvay, I. Mayer, Chem. Phys. Lett. 297 (1998) 365.
[72] T.R. Cundari, M.S. Gordon, J. Am. Chem. Soc. 113 (1991) 5231.
[73] T.R. Cundari, M.S. Gordon, Organometallics 11 (1992) 55.
[74] J.H. Oskam, R.R. Schrock, J. Am. Chem. Soc. 115 (1993) 11831.
[75] R.-S. Zhou, R.L. Snyder, Acta Crystallogr. B 47 (1991) 617.
[76] E.S. Davie, D.A. Whan, C. Kemball, J. Catal. 24 (1972) 272.
[77] P. Chaumont, C.S. John, J. Mol. Catal. 46 (1988) 317.
[78] W. Grünert, R. Feldhaus, K. Anders, E.S. Shpiro, Kh.M. Minachev, J. Catal. 120 (1989) 444.
[79] J. Handzlik, J. Ogonowski, in: Technologia chemiczna na przełomie wieków, Wydawnictwo Stałego Komitetu Kongresów Technologii Chemicznej, Gliwice, 2000, p. 149. (The abstract in 3rd Congress of Chemical Technology: The Chemical Technology at the Change of the Century. Abstracts of Lectures, Oral Communications and Posters, p. 44. A Publication of the Permanent Committee of the Congresses of Chemical Technology, Gliwice 2000).
[80] A.J. Moffat, A. Clark, J. Catal. 17 (1970) 264.
[81] B.N. Shelimov, I.V. Elev, V.B. Kazansky, J. Catal. 98 (1986) 70.
[82] L.J. Alvarez, J.F. Sanz, M.J. Capitan, M.A. Centeno, J.A. Odriozola, J. Chem. Soc., Faraday Trans. 89 (1993) 3623.
[83] A.A. Tsyganenko, P.P. Mardilovich, J. Chem. Soc., Faraday Trans. 92 (1996) 4843.
[84] A.N. Startsev, O.V. Klimov, E.A. Khomyakova, J. Catal. 139 (1993) 134.